Two- and three-loop anomalous dimensions of Weinberg's dimension-six CP-odd gluonic operator

Author(s):
de Vries, Jordy; Falcioni, Giulio; Herzog, Franz; Ruijl, Ben

Publication date:
2020-07-01

Permanent link:
https://doi.org/10.3929/ethz-b-000429148

Originally published in:
Physical Review D 102(1), https://doi.org/10.1103/PhysRevD.102.016010

Funding acknowledgement:
694712 - Automatization of perturbative QCD at very high orders (EC)

Two- and three-loop anomalous dimensions of Weinberg's dimension-six *CP*-odd gluonic operator

Jordy de Vries,[1,2] Giulio Falcioni,[3] Franz Herzog,[4] and Ben Ruijl[5]

[1]*Amherst Center for Fundamental Interactions, Department of Physics, University of Massachusetts, Amherst, Massachusetts 01003, USA*
[2]*RIKEN BNL Research Center, Brookhaven National Laboratory, Upton, New York 11973-5000, USA*
[3]*Higgs Centre for Theoretical Physics, School of Physics and Astronomy, The University of Edinburgh, Edinburgh EH9 3FD, Scotland, United Kingdom*
[4]*Nikhef Theory Group, Science Park 105, 1098 XG Amsterdam, Netherlands*
[5]*ETH Zürich, Rämistrasse 101, 8092 Zürich, Switzerland*

(Received 8 August 2019; accepted 17 June 2020; published 15 July 2020)

We apply a fully automated extension of the R^* operation capable of calculating higher-loop anomalous dimensions of n-point Green's functions of arbitrary, possibly nonrenormalizable, local quantum field theories. We focus on the case of the CP-violating Weinberg operator of the Standard Model effective field theory whose anomalous dimension is so far known only at one loop. We calculate the two-loop anomalous dimension in full QCD and the three-loop anomalous dimensions in the limit of pure Yang-Mills theory. We find sizable two-loop and large three-loop corrections, due to the appearance of a new quartic group invariant. We discuss phenomenological implications for electric dipole moments and future applications of the method.

DOI: 10.1103/PhysRevD.102.016010

I. INTRODUCTION

The absence of evidence for beyond-the-Standard Model (BSM) physics in high-energy proton-proton collisions at the LHC, and in large classes of low-energy precision measurements, all indicate that the scale of BSM physics (Λ) is significantly higher than the electroweak scale (v): $\Lambda \gg v \simeq 246$ GeV. In such a scenario, the effects of BSM physics at low energies $E \ll \Lambda$ can be described in terms of effective operators consisting of SM fields that obey the SM gauge and Lorentz symmetries [1–3]. The resulting framework is called the SM effective field theory (SMEFT). The SMEFT Lagrangian contains an infinite number of operators that can be ordered by their dimension. Effects of higher-dimensional operators on low-energy observables are suppressed by additional powers of E/Λ.

The connection between observables at (relatively) low energies and the SMEFT operators at the scale Λ, where the effective operators can be matched to specific UV-complete BSM models, is determined by renormalization-group equations (RGEs). The RGEs depend on anomalous dimensions that can be calculated in perturbation theory in an expansion in small coupling constants. The complete one-loop anomalous dimension matrix of dimension-six SMEFT operators has been obtained [4–6]. Already for dimension six, the number of operators is large and the general mixing structure of the RGEs is rather complex. It has been observed that the one-loop anomalous dimension matrix is almost holomorphic [7], but it is not clear whether this feature extends to higher order. Higher-order anomalous dimensions have been calculated for subsets of dimension-six operators [8–23], but due to the hard technical nature of the calculations the complete matrix is not known. Higher-order anomalous dimensions can be used to (i) improve the precision of SMEFT contributions to LHC processes or low-energy precision observables, (ii) study the convergence of the perturbative expansions, and (iii) investigate the structure of the SMEFT mixing pattern.

In this paper we extend the R^* operation to the framework of the SMEFT and develop an efficient and highly automated method to calculate higher-order QCD anomalous dimensions of SMEFT operators. The R^* operation provides a way to subtract UV and IR divergences from Euclidean Feynman diagrams, taking care of the combinatorics of overlapping divergences [24–26]. Recently, it has been extended to Feynman diagrams with arbitrary numerator structure [27]. So far the R^* operation has been used extensively in calculations of anomalous dimensions in QCD; see, e.g., [28–31]. However, the R^*

method is not limited to pure QCD and can be applied to arbitrary local quantum field theories.

To avoid the complicated mixing structure of SMEFT operators, we focus on a specific SMEFT dimension-six operator. Once tested and developed, the method can be extended to a larger set of operators without too many additional complications. The operator we now consider is the CP-violating gluonic operator, often called "the Weinberg operator" [32], defined as

$$\mathcal{L}_6 = \frac{C_W}{6} f^{abc} \epsilon^{\mu\nu\alpha\beta} G^a_{\alpha\beta} G^b_{\mu\rho} G^{c\rho}_{\nu} \equiv C_W O_W, \tag{1}$$

in terms of the gluon field strength $G^a_{\alpha\beta}$, the Levi-Civita tensor (LCT) $\epsilon^{\mu\nu\alpha\beta}$, the gauge group structure constants f^{abc}, and the Wilson coefficient $C_W \sim 1/\Lambda^2$. The Weinberg operator is induced in various classes of BSM models with additional CP-violating phases such as supersymmetric models, two-Higgs doublet models, and models with leptoquarks [33–35]. The Weinberg operator is also induced from dimension-six CP-odd operators in the SMEFT Lagrangian involving heavy quarks, prominent examples being heavy-quark chromoelectric dipole moments [36,37], and heavy-quark Yukawa interactions [36,38,39]. At lower energies, the Weinberg operator leads to nonzero electric dipole moments (EDMs) of nucleons, nuclei, and diamagnetic atoms (such as ^{199}Hg [40]). Current experimental EDM limits [41] set strong constraints on BSM models that induce the Weinberg operator.

To use EDM limits to constrain the Weinberg operator, and the associated BSM models, it is necessary to evolve the Weinberg operator from the high-energy scale where it is induced to the low-energy scale where the Weinberg operator is matched to hadronic CP-violating operators. This evolution is determined by the anomalous dimension of the Weinberg operator. The one-loop anomalous dimension of the Weinberg operator was obtained in the original paper by Weinberg [32], albeit with the wrong sign, finding sizable QCD corrections from the evolution of C_W from high- to low-energy scales. The calculation was corrected in Refs. [42–44] that also calculated the mixing, proportional to the small quark masses, of the Weinberg operator into the quark chromoelectric dipole moment. The only other operator C_W can mix with is the QCD theta term $\sim\epsilon^{\mu\nu\alpha\beta} G^a_{\alpha\beta} G^a_{\mu\nu}$, but this mixing is of little phenomenological use as the bare theta term is an unknown SM parameter. Furthermore, the renormalized theta term vanishes after a Peccei-Quinn mechanism [45]. We will not consider the mixing into the theta term in this paper.

The potential phenomenological implications of the unknown higher-loop anomalous dimensions of C_W, in addition to the high complexity of the Feynman rules induced by the Weinberg operator, make determining the higher-order corrections a suitable real-world test case for the R^* method.

II. THE BACKGROUND-FIELD METHOD

The renormalization of Green's functions with a single insertion of the Weinberg operator O_W requires in general a counterterm matrix Z_{ij}. The matrix Z_{ij} takes into account mixing with all the operators of equal or smaller mass dimension, which share the same quantum numbers as O_W [46,47]:

$$O^R_W = \sum_j Z_{Wj} O^B_j. \tag{2}$$

The operators that contribute to Eq. (2) are divided into three classes [48,49]:

(i) gauge invariant (GI) physical operators,
(ii) operators that vanish after applying the classical equations of motion (EOM), and
(iii) Becchi-Rouet-Stora-Tyutin (BRST)-exact operators.

The EOM and the BRST-exact operators are unphysical, since they have vanishing S-matrix elements. Nevertheless they have nonzero Green's functions and associated UV counterterms which mix with O_W, as in Eq. (2).

We use the background-field method [50–53] to simplify the mixing pattern of Eq. (2). The main advantage of this method is that it preserves gauge invariance of the background field, so that the UV counterterms of 1PI correlators of the background fields involve only GI operators. This feature puts strong constraints on the nonphysical operators in Eq. (2): BRST-exact operators will not contribute to the UV counterterms and gauge invariance will restrict EOM operators too. For example, in Yang-Mills theory without fermions ($n_f = 0$), there is only one independent gauge invariant EOM operator

$$\tilde{O}_E = \frac{1}{4} \epsilon^{\mu_1\mu_2\mu_3\mu_4} (D_{\mu_1} G_{\mu_2\mu_3})^a (D^\lambda G_{\lambda\mu_4})^a, \tag{3}$$

where D^a_μ is the covariant derivative. However, $\tilde{O}_E$ vanishes by the Bianchi identity. Therefore it is impossible to construct purely gluonic unphysical operators mixing with O_W. In the rest of this paper, we will compute directly the UV counterterm Z_{WW}, which cancels the local UV divergences of the background-field correlators with a single O_W vertex. The R^* operation, which subtracts recursively all the UV subdivergences of the diagrams in a fully automated way, will be the key tool to isolate the gauge invariant local UV divergence of the correlators. We calculate Z_{WW} at the two-loop level in full QCD. At three loops, we only consider Z_{WW} in Yang-Mills theory without fermions. The corresponding diagrams are the most computationally demanding. In general, the inclusion of fermions will also generate off-diagonal mixing Z_{Wj} with quark (chromo) electric operators [54,55]. These contributions will be the subject of a separate work.

III. THE R^* OPERATION FOR GENERAL FEYNMAN DIAGRAMS

The renormalization constant Z_{WW} can be extracted from the 1PI correlator Γ_W^{nb} of n background fields with a single insertion of O_W—see Fig. 1 for examples of Feynman diagrams—by acting on it with the UV-counterterm operation $\mathcal{Z}$:

$$Z_{WW}Z_b^{3/2}O_W^{nb}(C_W;p_1,\ldots,p_n) = \mathcal{Z}(\Gamma_W^{nb}(\alpha_s,C_W;p_1,\ldots,p_n)), \tag{4}$$

where Z_b is the well-known wave function renormalization of the background gauge field [52,53] and the $\mathcal{Z}$ operation is defined to include counterterms for all the UV subdivergences of Γ_W^{nb}. Here O_W^{nb} denotes the Feynman rule of the n background-field vertex generated by the Weinberg operator. The calculation of renormalization constants can be simplified by nullifying the external momenta of Γ_W^{nb} after applying a Taylor expansion in the external momenta whose order equals the superficial degree of divergence of the correlator; for the case of Γ_W^{nb} this is $\omega(\Gamma_W^{nb}) = 6-n$, e.g., $\omega(\Gamma_W^{3b}) = 3$. After the external momenta are nullified, a convenient scale can be reintroduced into the correlator by introducing either arbitrarily chosen external momenta into each Feynman diagram or inserting a mass into a single propagator. This is known as the procedure of infrared rearrangement (IRR) [56]. Nullifying the external momenta introduces new IR divergences, which are fully automatically subtracted by the local R^* operation.

In contrast to earlier works which made use of the R^* operation, we now act it on Feynman diagrams before contracting any of the Feynman rules. This makes the algorithm more efficient and allows us to directly compute the UV counterterm of a particular diagram in $\overline{\text{MS}}$. As discussed in Ref. [27], this is not possible if the Feynman rules are contracted before the action of R^*. The algorithm of [27] was therefore only capable of extracting the pole terms of self-energy diagrams from simpler self-energy diagrams. The more general method used in this work allows us to reduce the calculation of UV counterterms of correlators with arbitrary numbers of external legs to the calculation of massless self-energy diagrams of one loop less. Therefore, this method has quite some advantages compared to the former, but its implementation introduces new complications. For instance, the Taylor expansion must be applied before the contraction of the Feynman rules, which leads to a new set of "differentiated" Feynman rules (essentially new vertices and propagators). A more detailed overview of the method will be given in an upcoming publication [57]. Employing this new formalism we write

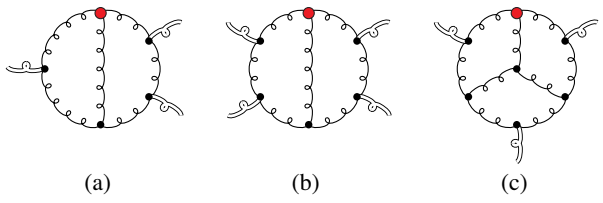

FIG. 1. Two-loop diagrams with three (a) and four (b) external background fields and a three-loop diagram with three external background fields (c). Gluons are denoted by curly lines and an insertion of the Weinberg operator by a red dot.

$$\mathcal{Z}(\Gamma_W^{nb}) = -K\bar{R}^*(\mathcal{T}^{(6-n)}_{p_1,\ldots,p_n}\Gamma_W^{nb}|_{p_i=0}), \tag{5}$$

where the operation $\bar{R}^*$ acting on a Feynman diagram Γ subtracts from it counterterms for all UV subdivergences and all IR divergences. The operation K extracts the single- and multipole contributions in the dimensional regulator $\epsilon = (4-D)/2$ and $\mathcal{T}^{(\omega)}_{p_1,\ldots,p_n}$ denotes the Taylor expansion operator for the order ω term in the expansion around the (external) momenta $p_1,\ldots,p_n$. More precisely (although we leave the nitty gritty of the graph combinatorics to the literature; see, e.g., [27] or [58]), the $\bar{R}^*$ is defined as

$$\bar{R}^*(\Gamma) = \sum_{\gamma\cap\tilde{\gamma}=\emptyset'} \tilde{\mathcal{Z}}(\tilde{\gamma}) * \mathcal{Z}(\gamma) * \Gamma\backslash\tilde{\gamma}/\gamma, \tag{6}$$

where the sum goes overall nonintersecting UV subgraphs γ (but not including the full graph Γ) and IR subgraphs $\tilde{\gamma}$ (including also Γ in the case that Γ is a log-divergent vacuum graph). The operation $\tilde{\mathcal{Z}}$ here is the IR-counterterm operation which can always be rewritten in terms of the UV-counterterm operation of $\tilde{\gamma}$ and its subgraphs. The remaining contracted graph $\Gamma\backslash\tilde{\gamma}/\gamma$ is constructed by deleting the IR subgraph and then contracting the UV subgraph to a point. The $*$ operation denotes insertion of the counterterms into the remaining contracted graph; it reduces to the usual multiplication for log-divergent counterterms.

To simplify the calculation of the counterterm we use the fact that the $\mathcal{Z}$ operation commutes with the Taylor expansion operator. In the following we give some examples of this procedure. Let us start with the calculation of the UV counterterm of the following one-loop graph:

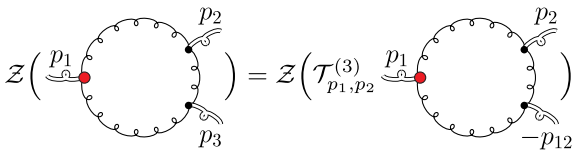

(7)

Here the thicker red vertex continues to denote the Weinberg operator. The Taylor expansion operator has to applied before the contraction of the Feynman rules. This procedure can be carried out diagrammatically, after choosing a momentum routing. Here we pick p_1 and p_2 as independent external momenta and write

$p_3 = -p_1 - p_2 = -p_{12}$. To simplify the derivative calculation it is usually best to pick the shortest paths through the diagram. Subsequently one differentiates along the path using nothing but the product and chain rule; thereby one generates a (potentially large) sum of new diagrams which contain differentiated propagators and vertices and with the external momenta nullified.

We graphically depict the differentiated vertex or Feynman rule with a small line $\multimap p$, and a label denoting that the momentum p has been differentiated with operator $p.\partial_p$. The orientation of the derivative fixes the direction of the path. Subsequently we need to nullify the external momenta; we introduce an encircled vertex ⊙ to denote that the external momentum (in our case always associated to the background field) has been nullified. Naturally both nullification and derivation will also occur simultaneously on certain vertices. In this case the expression is to be understood as $p.\partial_p(\bullet)|_{p=0}$. After the derivations, external momentum nullifications and mass insertions have been carried out we then obtain (writing just a few terms)

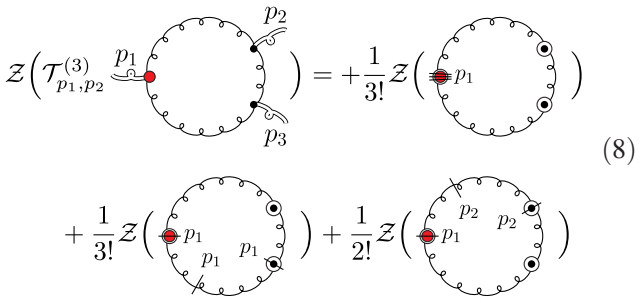

(8)

To evaluate one of the counterterms we need to introduce a scale back into the vacuum diagrams. Given that they are logarithmically divergent, the counterterms are independent of all scales. A simple choice is to insert a mass into a single propagator, denoted graphically by a thicker line. When possible it is convenient to insert the mass in such a way as to prevent IR divergences from occurring. Let us consider just the first term on the right-hand side of Eq. (8). A possible IR rearrangement to avoid the IR divergence is

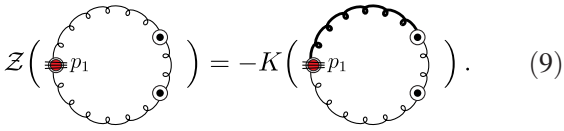

(9)

The absence of infrared singularities in the rearranged diagram of Eq. (9) is verified by applying a power counting procedure in the infrared region of the loop momentum, characterized by $k^\mu \to \lambda k^\mu$ with $\lambda \ll 1$. In this limit, each massless propagator diverges as $\mathcal{O}(\frac{1}{\lambda^2})$. However, each vertex provides a suppression in the numerator, given, respectively, by

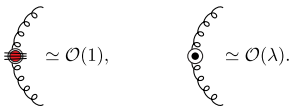

(10)

Therefore, the infrared region gives a vanishing contribution to the diagram

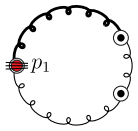

(11)

An IR counterterm would have been required had we used instead

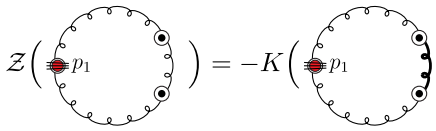

(12)

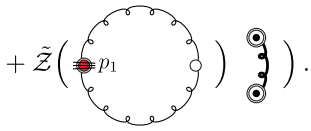

(13)

Here we introduced a doubly encircled vertex, which corresponds to a single encircled vertex with a further gluon's momentum nullified. Such a vertex vanishes in fact, and so for this reason the counterterm would not survive. Let us nevertheless continue with its evaluation to give an example of the procedure. The IR counterterm can be evaluated by relating it to a UV counterterm; this procedure has been used extensively in the R^* literature for scalar diagrams and we straightforwardly extend it to the nonscalar case. Here we can do this as follows:

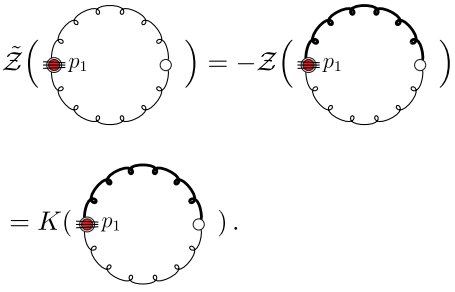

(14)

Having introduced the basic concepts let us now illustrate the procedure for the evaluation of a suitably differentiated and IR-rearranged two-loop diagram:

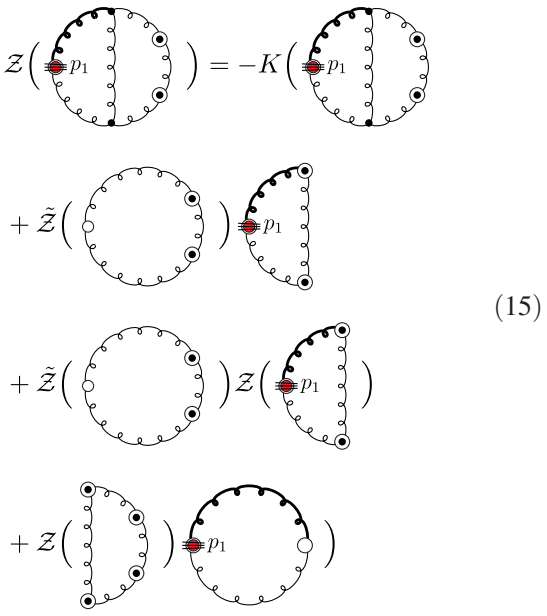

(15)

This diagram requires several counterterms, some of which we discard immediately due to scalelessness of the remaining or contracted graphs. The second term on the right-hand side captures a one-loop IR subdivergence. The third term has the same IR divergence with the remaining graph also giving rise to a UV subdivergence. The last term corresponds to another UV subdivergence, which was originally of box type.

IV. CALCULATION AND RESULTS

The actual calculation of the Feynman diagrams contributing to Γ_W^{nb}, which we first generate using QGRAF [59], is done via two independent codes. The Levi-Civita tensor appearing in the Weinberg operator is not strictly defined in D dimensions and one must fix a scheme when encountering it within dimensional regularization. In the first code, written in MAPLE, we use the Larin [60] scheme for the LCT appearing in the Feynman rules. The second code is written in FORM [61] and applies the 't Hooft-Veltman (HV) scheme [62]. The implementation of these schemes is further discussed in the Appendix. Since the implementation of these two schemes results in rather different algorithms, obtaining a consistent result provides a powerful check. For the reduction to master integrals both our implementations heavily rely on the FORCER program [63].

To calculate the two- and three-loop anomalous dimensions of the Weinberg operator one can extract Z_W from the correlator Γ_W^{nb} for $n = 3$–6. Ward identities ensure that the resulting anomalous dimension is independent of n. A smaller n implies a lower number of diagrams to compute. However, this is counterbalanced by the fact that the n-background field correlator must be differentiated $6-n$ times with respect to external momenta in order for IRR to be applicable. Even though the Taylor expansion proliferates terms for the $n = 3$ case, it is nevertheless the least computationally demanding and involves 250 diagrams. At the two-loop level we obtain the result

$$Z_{WW}(2-\text{loop}) = \left(\frac{\alpha_s}{4\pi}\right)^2 \left[C_A^2\left(-\frac{19}{24\epsilon^2}+\frac{119}{36\epsilon}\right) - C_A n_f T_f\left(\frac{7}{3\epsilon^2}+\frac{4}{3\epsilon}\right) + \frac{3C_F n_f T_f}{\epsilon}+\frac{10 n_f^2 T_f^2}{3\epsilon^2}\right], \tag{16}$$

where C_A is the adjoint Casimir, $C_A = N_c$ for the gauge group $\mathrm{SU}(N_c)$, with N_c the number of colors.

We have checked our two-loop results in four ways. First, as discussed above we have applied two independent codes to the $n_f = 0$ terms, obtaining the same result. Second, in the form code we investigated gauge invariance by performing the computation with a single power of the gauge parameter ξ^1 and verified that it cancels. Third, we have extracted Z_{WW} from the $n = 4$ case. The evaluation of the associated 2389 diagrams leads to the same two-loop result for Z_{WW}. Finally, the $1/\epsilon^2$ poles can be determined from one-loop results, and we have verified that our results match the one-loop predictions.

Using the form code, which is optimized for large expressions, we evaluated the $n_f = 0$ three-loop correction to Z_{WW}. This required the computation of 6203 diagrams involving up to $\mathcal{O}(10^9)$ terms in intermediate expressions. The total computation time came to 48 h on a 24-core machine with 2.4 GHz Intel Xeon E5-2695v2 CPUs and 150 GB of memory, whereas the two-loop computation only took 20 min. We obtain the result

$$Z_{WW}(3\text{-loop}) = \left(\frac{\alpha_s}{4\pi}\right)^3 \left\{C_A^3\left[\frac{779}{432\epsilon^3}-\frac{5389}{648\epsilon^2}-\frac{3203}{1944\epsilon} + \frac{44\zeta_3}{3\epsilon}\right] + \frac{d_A^{abcd}d_A^{abcd}}{N_A C_A}\left[\frac{40}{3\epsilon}-\frac{352\zeta_3}{\epsilon}\right]\right\}. \tag{17}$$

Here we encounter the Riemann zeta value $\zeta_3 \simeq 1.202$ and the quartic Casimir $d_A^{abcd}d_A^{abcd}/(N_A C_A)$; see Ref. [64] for more details. For $\mathrm{SU}(N_c)$ this becomes $d_A^{abcd}d_A^{abcd}/(N_A C_A) = N_c(N_c^2+36)/24$. We checked this result by verifying that the $1/\epsilon^2$ and $1/\epsilon^3$ poles match one- and two-loop predictions. Furthermore, the fact that Z_{WW} is proportional to the three-gluon Feynman rule of the Weinberg operator is another nontrivial cross-check.

V. DISCUSSION

The UV counterterm determines the anomalous dimension of the Weinberg operator up to three loops:

$$\gamma_{WW} = \frac{\alpha_s(\mu^2)}{4\pi}\left[\frac{C_A}{2} + 2n_f T_f\right] + \left(\frac{\alpha_s(\mu^2)}{4\pi}\right)^2\left[\frac{119}{18}C_A^2 + n_f T_f\left(6C_F - \frac{8C_A}{3}\right)\right] + \left(\frac{\alpha_s(\mu^2)}{4\pi}\right)^3\left[C_A^3\left(-\frac{3203}{648} + 44\zeta_3\right) + \frac{d_A^{abcd}d_A^{abcd}}{N_A C_A}(40 - 1056\zeta_3) + \mathcal{O}(n_f)\right], \quad (18)$$

where we included the complete dependence on n_f, the number of active quark flavors, at one and two loops. Remarkably the two-loop n_f dependence drops out since $C_F = 4/3$ and $C_A = 3$ for $N_c = 3$. This is an accidental cancellation for $N_c = 3$ but even for a larger number of colors the n_f corrections are negligible due to the large prefactor of the C_A^2 term. It is interesting that ζ_3 and the quartic group invariant enter at three loops, unlike the QCD beta function where they appear only at the four-loop order. However, to the best of our knowledge, there is nothing that forbids their appearance at lower order in the Weinberg operator. We notice that the coefficient of the quartic group invariant is directly proportional, up to a factor $2C_A/9$, to the same quartic group invariant appearing in the four-loop QCD beta function. While this could simply be a coincidence, it would be interesting to see if similar patterns appear at higher loop orders. Finally, we have not calculated the n_f corrections at three loops, but if a similar pattern appears as at two loops, then neglecting their contributions would provide a good approximation.

In order to estimate the impact of the two- and three-loop contributions to the anomalous dimension we set $C_A = 3$, $C_F = \frac{4}{3}$ and $n_f = 0$ in Eq. (18) and we obtain the series

$$\frac{8\pi\gamma_{WW}}{\alpha_s(\mu^2)C_A} = 1 + 3.15657\alpha_s - 23.72872\alpha_s^2. \quad (19)$$

The next-to-next-to-leading-order (NNLO) coefficient can be decomposed as $23.72872 = 5.46537 - \underline{29.19409}$, where the underlined number stems from the contribution of the quartic group invariant, which is responsible for the large negative correction. The size of the coefficients increases drastically with the loop order and undermines the convergence of the α_s expansion, unless large cancellations occur in the n_f-dependent pieces of the three-loop anomalous dimensions that are not computed in this work.

As an example, we calculate the evolution of C_W, determined by

$$\mu^2\frac{dC_W(\mu)}{d\mu^2} = \gamma_{WW}C_W(\mu), \quad (20)$$

TABLE I. Evolution factors at different perturbative orders that relate $C_W(\mu)$ to $C_W(1\ \text{TeV})$.

μ[GeV]	LO	NLO	NNLO
100	0.76	0.75	0.76
5	0.48	0.44	0.48
2	0.39	0.34	0.40
1	0.33	0.26	0.37

from a specific high-energy scale $\mu_H = 1$ TeV, where we assume $C_W(\mu_H) = 1$, to various low-energy scales. We use $\alpha_s(M_Z) = 0.118$ and $M_Z = 91.2$ GeV [65], and apply the QCD beta function at two [66–68] and three loops [69,70]. When evaluating the beta function we adjust the number of fermions n_f at the top, bottom and charm thresholds:

$$m_t(m_t) = 160\ \text{GeV}, \qquad m_b(m_b) = 4.18\ \text{GeV}, \qquad m_c(m_c) = 1.28\ \text{GeV}. \quad (21)$$

The Wilson coefficient at the different energy scales is given in Table I, where we kept the LO and NLO n_f dependence. Around and above the electroweak scale, α_s is sufficiently small such that NLO and NNLO corrections are suppressed. For $\mu \leq 100$ GeV, NNLO corrections are as large as, or larger than, NLO corrections. At lower energies higher orders become relevant, and in particular for $\mu = 1$ GeV, the scale where the Weinberg operator is often matched to hadronic quantities, the NLO and NNLO correction are -21% and $+33\%$ of the LO result, respectively. The total result, however, is not far from the LO result due to cancellations between NLO and NNLO corrections. The lack of convergence is worrying and warrants a four-loop calculation.

The main phenomenological impact of a nonzero Weinberg operator is its contribution to the neutron EDM d_n. The QCD matrix element connecting d_n to C_W is difficult to calculate, but future lattice-QCD calculations might be up to the task [71–73]. Two techniques have been used to estimate the matrix element. A QCD sum-rule estimate [33,74] gives $d_n = (25 \pm 12)$ MeV $eC_W(1\ \text{GeV})$. Another technique that is often applied is naive dimensional analysis (NDA) [75]. NDA predicts [32,76]

$$|d_n| \simeq e\frac{\Lambda_\chi}{4\pi}C_W(\mu_{\text{match}}), \quad (22)$$

where $\Lambda_\chi \simeq 1.2$ GeV denotes the chiral-symmetry-breaking scale and μ_{match} a matching scale at hadronic energies. Unlike the QCD sum rules calculation, the NDA estimate is sensitive to the evolution of the Weinberg operator to the low hadronic matching scale. Which scale to pick is unclear, but typically the scale where $\alpha_s(\mu_{\text{match}}) = 2\pi/3$ is applied as suggested by Weinberg [32]. Using one-loop evolution this leads to $|d_n^{\text{LO}}| \simeq e40$ MeV $C_W^{\text{LO}}(1\ \text{GeV})$ in reasonable agreement with QCD sum rules as pointed out in [33]. However, the large NNLO corrections significantly

affect the running in the nonperturbative regime and lead to much larger estimates $|d_n^{\mathrm{NNLO}}| \simeq e1\ \mathrm{GeV}\, C_W^{\mathrm{LO}}(1\ \mathrm{GeV})$, indicating that NDA estimates are not stable. We therefore recommend the use of QCD sum rules [33,74], which only depend on the evolution to the perturbative scale $\mu_L \simeq 1$ GeV. Ideally, these calculations are replaced by lattice-QCD results in the future [71–73,77].

Using the conservative QCD sum rule expression $d_n = 13\ \mathrm{MeV}\, eC_W(1\ \mathrm{GeV})$, and our result for the anomalous dimension, the current neutron EDM limit, $d_n < 1.8 \times 10^{-13}$ e fm [78] can be used to constrain the Weinberg operator. We write $C_W(\Lambda) = d_W(\Lambda)/\Lambda^2$, where $d_W(\Lambda)$ is a dimensionless constant. For $\Lambda = 1$ TeV, we obtain the constraint $d_W(1\ \mathrm{TeV}) < \{2.1, 2.7, 1.9\} \times 10^{-4}$, where the results in brackets are obtained with the LO, NLO, and N^{2}LO anomalous dimension, respectively. The limits are rather stringent, in particular in comparison with limits on the CP-even counterpart of the Weinberg operator

$$\mathcal{L}_6 = \frac{c_G}{\Lambda^2} f^{abc} G_\nu^{a,\rho} G_\lambda^{a,\nu} G_\rho^{c,\lambda}, \tag{23}$$

that is constrained at the percent level $c_G(1\ \mathrm{TeV}) \leq 4 \times 10^{-2}$ from an analysis of multijet production at the LHC [79].

VI. CONCLUSION

In this paper we have reported a new method to calculate higher-order QCD anomalous dimensions of SMEFT operators in a highly automated manner. To develop and test the method we focused on one particular operator, the CP-violating gluonic Weinberg operator, whose anomalous dimension is hard to calculate, even at one loop [32,42–44]. Due to its CP-violating nature this operator does not mix into lower-dimensional operators containing just gauge fields. By also applying the background-field method, we avoid complications associated to operator mixing. We extracted the two-loop anomalous dimension by calculating 250 diagrams contributing to the three-background-gluon vertex. We verified our result by extracting the same anomalous dimension of the 2389 diagrams contributing to the four-background-gluon vertex, as predicted by gauge invariance. Finally, due to the automated nature of the framework we were able to immediately calculate the three-loop anomalous dimension at $n_f = 0$ by evaluating 6203 diagrams.

We found a sizable positive two-loop correction to the anomalous dimension, which turns out to be independent on n_f, the number of flavors, due to an accidental cancellation for $N_c = 3$. Even at $N_c \neq 3$, the n_f-dependent corrections are negligible. We proceeded to calculate the three-loop correction in $n_f = 0$ limit and found a negative contribution, which is sufficiently large to threaten the perturbative convergence, as the two- and three-loop evolution factors almost cancel. The lack of convergence motivates a calculation of the four-loop anomalous dimension and the missing three-loop n_f corrections.

The R^* operation combined with the background-field method provides a powerful framework for higher-order loop calculations, and our calculation can be extended into several directions without too much additional effort. In fact, our setup works up to five loops. Currently the only hurdle is computing time. Beyond five loops—should the need for such corrections ever arise—there exists neither a complete basis of master integrals nor a suitable reduction onto such a basis. However, the R^* operation itself is valid to all loop orders.

So far, we have only performed higher-order loop calculations for operator without external quarks, and the framework must be extended to renormalize SMEFT operators containing quark fields. There are no inherent additional complications associated to the inclusion of quarks, but a consistent treatment of γ^5 in the R^* method needs to be developed. This is left to future work. Here we have taken a first big step by presenting methods for the consistent use of LCTs beyond one loop in both the Larin and HV schemes. Once developed, we can calculate the (so far unknown) higher-loop mixing of the Weinberg operator into the quark electric and chromoelectric dipole moments and CP-odd four-quark operators. It would also be interesting to compute four-loop corrections to the anomalous dimension, to see whether the trend of large coefficients continues and whether other surprising relations, such as the one found for the quartic group invariants, to the QCD beta function appear.

While this work focused on the Weinberg operator, this is by no means an inherent limitation of the method. We envision calculations of higher-order anomalous dimensions of a much larger class of SMEFT operators. Isolating the footprints of SMEFT operators left behind at the LHC, or future colliders, from SM contributions is an active field of research [80,81]. Higher-order QCD corrections to SMEFT contributions can be sizable, as shown here, and are important to disentangle SMEFT operators [82]. Higher-loop anomalous dimensions will further reduce theoretical uncertainties and make the theoretical framework of the SMEFT more robust.

ACKNOWLEDGMENTS

We are grateful for conversations with Emanuele Mereghetti, Sven Moch, Giovanni Marco Pruna, Adam Ritz, Peter Stoffer, Jos Vermaseren and Stefano di Vita. The research of F. H. is supported by the NWO Vidi Grant No. 680-47-551. J. d. V. is supported by the RHIC Physics Fellow Program of the RIKEN BNL Research Center. G. F. received support from the ERC Advanced Grant No. 320651, "HEPGAME." The research of B. R. is supported by the ERC Advanced Grant No. 694712, "PertQCD."

APPENDIX: LEVI-CIVITA SYMBOLS AND THE R^* METHOD

We define the LCTs in the respective schemes by $\varepsilon_{HV}^{\mu_1\ldots\mu_4}$ and $\varepsilon_L^{\mu_1\ldots\mu_4}$. While ε_{HV}, associated to the HV scheme [62], lives in the four-dimensional subspace, ε_L, associated to the Larin scheme [60], has components in the full D-dimensional space. As such, we can freely commute ε_{HV} with the pole operation K which appears in the R^*-counterterm operation:

$$K(\varepsilon_{HV}^{\mu_1\ldots\mu_4} F_{\mu_1\ldots\mu_4\ldots}) = \varepsilon_{HV}^{\mu_1\ldots\mu_4} K(F_{\mu_1\ldots\mu_4\ldots}). \tag{A1}$$

A simple, although inefficient, procedure to use the local R^* operation in the HV scheme is to commute ε_{HV} out of all the potentially nested Ks and then to apply a standard tensor reduction on the remaining tensor as described in Ref. [83]. In the Larin scheme Eq. (A1) does not hold and we apply a different procedure. To compute the expression

$$K(F_\varepsilon^{\nu_1\ldots\nu_n}) = K(\varepsilon_L^{\mu_1\ldots\mu_4} F_{\mu_1\ldots\mu_4}^{\nu_1\ldots\nu_n}), \tag{A2}$$

we first tensor-reduce the object $F_\varepsilon^{\nu_1\ldots\nu_n}$, which (assuming that the object is superficially log divergent) can be reduced in terms of $\varepsilon_L^{\mu_1\ldots\mu_4}$ and metric tensors $g^{\mu_1\mu_2}$. We thus write

$$K(F_\varepsilon^{\nu_1\ldots\nu_n}) = \sum_\sigma T_\sigma^{\nu_1\ldots\nu_n} K(F_\varepsilon^\sigma), \tag{A3}$$

where

$$T_\sigma^{\nu_1\ldots\nu_n} = \varepsilon_L^{\nu_{\sigma(1)}\ldots\nu_{\sigma(4)}} g^{\nu_{\sigma(5)}\nu_{\sigma(6)}}\ldots g^{\nu_{\sigma(n-1)}\nu_{\sigma(n)}}, \tag{A4}$$

and the sum goes over all permutations of the indices which do not leave the tensor structure invariant. The coefficients F_ε^σ are defined

$$F_\varepsilon^\sigma = P^\sigma_{\nu_1\ldots\nu_n} F_\varepsilon^{\nu_1\ldots\nu_n}, \tag{A5}$$

where the projector P^σ satisfies

$$P^\sigma_{\nu_1\ldots\nu_n} T_\tau^{\nu_1\ldots\nu_n} = \delta_{\sigma\tau} \tag{A6}$$

and $\delta_{\sigma\tau}$ is a Kronecker delta which yields 1 if the two permutations τ and σ are identical and 0 otherwise. The P^σ themselves can be constructed as linear combinations of T_σ's. Using the identity

$$\varepsilon_L^{\nu_1\ldots\nu_4}\varepsilon_L^{\mu_1\ldots\mu_4} = \det\begin{pmatrix} g^{\mu_1\nu_1} & g^{\mu_1\nu_2} & \ldots & g^{\mu_1\nu_4} \\ g^{\mu_2\nu_1} & g^{\mu_2\nu_2} & \ldots & g^{\mu_2\nu_4} \\ \ldots & \ldots & \ldots & \ldots \\ g^{\mu_4\nu_1} & g^{\mu_4\nu_2} & \ldots & g^{\mu_4\nu_4} \end{pmatrix}, \tag{A7}$$

products of two LCTs in the Larin scheme can always be evaluated in terms of D-dimensional metric tensors. The scalar functions F_ε^σ are thus functions of D-dimensional scalar products only and therefore may never contain any LCTs.

[1] W. Buchmüller and D. Wyler, Effective Lagrangian analysis of new interactions and flavor conservation, Nucl. Phys. **B268**, 621 (1986).

[2] B. Grzadkowski, M. Iskrzynski, M. Misiak, and J. Rosiek, Dimension-six terms in the standard model Lagrangian, J. High Energy Phys. 10 (2010) 085.

[3] I. Brivio and M. Trott, The standard model as an effective field theory, Phys. Rep. **793**, 1 (2019).

[4] E. E. Jenkins, A. V. Manohar, and M. Trott, Renormalization group evolution of the standard model dimension six operators I: Formalism and lambda dependence, J. High Energy Phys. 10 (2013) 087.

[5] E. E. Jenkins, A. V. Manohar, and M. Trott, Renormalization group evolution of the standard model dimension six operators II: Yukawa dependence, J. High Energy Phys. 01 (2014) 035.

[6] R. Alonso, E. E. Jenkins, A. V. Manohar, and M. Trott, Renormalization Group evolution of the standard model dimension six operators III: Gauge coupling dependence and phenomenology, J. High Energy Phys. 04 (2014) 159.

[7] R. Alonso, E. E. Jenkins, and A. V. Manohar, Holomorphy without supersymmetry in the standard model effective field theory, Phys. Lett. B **739**, 95 (2014).

[8] G. Altarelli, G. Curci, G. Martinelli, and S. Petrarca, QCD nonleading corrections to weak decays as an application of regularization by dimensional reduction, Nucl. Phys. **B187**, 461 (1981).

[9] A. J. Buras and P. H. Weisz, QCD nonleading corrections to weak decays in dimensional regularization and 't Hooft-Veltman schemes, Nucl. Phys. **B333**, 66 (1990).

[10] A. J. Buras, M. Jamin, M. E. Lautenbacher, and P. H. Weisz, Effective Hamiltonians for $\Delta S = 1$ and $\Delta B = 1$ nonleptonic decays beyond the leading logarithmic approximation, Nucl. Phys. **B370**, 69 (1992); **B375**, 501(A) (1992).

[11] M. Ciuchini, E. Franco, G. Martinelli, and L. Reina, ϵ'/ϵ at the next-to-leading order in QCD and QED, Phys. Lett. B **301**, 263 (1993).

[12] M. Ciuchini, E. Franco, G. Martinelli, and L. Reina, The delta $S = 1$ effective Hamiltonian including next-to-leading order QCD and QED corrections, Nucl. Phys. **B415**, 403 (1994).

[13] M. Misiak and M. Munz, Two loop mixing of dimension five flavor changing operators, Phys. Lett. B **344**, 308 (1995).

[14] K. G. Chetyrkin, M. Misiak, and M. Munz, Weak radiative B meson decay beyond leading logarithms, Phys. Lett. B **400**, 206 (1997); Erratum, Phys. Lett. B **425**, 414 (1998).

[15] K. G. Chetyrkin, M. Misiak, and M. Munz, Beta functions and anomalous dimensions up to three loops, Nucl. Phys. **B518**, 473 (1998).

[16] M. Ciuchini *et al.*, Delta M(K) and epsilon(K) in SUSY at the next-to-leading order, J. High Energy Phys. 10 (1998) 008.

[17] A. J. Buras, M. Misiak, and J. Urban, Two loop QCD anomalous dimensions of flavor changing four quark operators within and beyond the standard model, Nucl. Phys. **B586**, 397 (2000).

[18] J. A. Gracey, Three loop MS-bar tensor current anomalous dimension in QCD, Phys. Lett. B **488**, 175 (2000).

[19] P. Gambino, M. Gorbahn, and U. Haisch, Anomalous dimension matrix for radiative and rare semileptonic B decays up to three loops, Nucl. Phys. **B673**, 238 (2003).

[20] M. Gorbahn and U. Haisch, Effective Hamiltonian for non-leptonic $|\Delta F| = 1$ decays at NNLO in QCD, Nucl. Phys. **B713**, 291 (2005).

[21] M. Gorbahn, U. Haisch, and M. Misiak, Three-Loop Mixing of Dipole Operators, Phys. Rev. Lett. **95**, 102004 (2005).

[22] G. Degrassi, E. Franco, S. Marchetti, and L. Silvestrini, QCD corrections to the electric dipole moment of the neutron in the MSSM, J. High Energy Phys. 11 (2005) 044.

[23] M. Czakon, U. Haisch, and M. Misiak, Four-loop anomalous dimensions for radiative flavour-changing decays, J. High Energy Phys. 03 (2007) 008.

[24] K. G. Chetyrkin and F. V. Tkachov, Infrared R operation and ultraviolet counterterms in the MS scheme, Phys. Lett. **114B**, 340 (1982).

[25] K. G. Chetyrkin, Combinatorics of **R**-, $\mathbf{R}^{-1}$-, and $\mathbf{R}^{*}$-operations and asymptotic expansions of feynman integrals in the limit of large momenta and masses, arXiv: 1701.08627.

[26] K. G. Chetyrkin and V. A. Smirnov, R* operation corrected, Phys. Lett. **144B**, 419 (1984).

[27] F. Herzog and B. Ruijl, The R^{*}-operation for Feynman graphs with generic numerators, J. High Energy Phys. 05 (2017) 037.

[28] P. A. Baikov, K. G. Chetyrkin, and J. H. Kühn, Five-Loop Running of the QCD Coupling Constant, Phys. Rev. Lett. **118**, 082002 (2017).

[29] F. Herzog, B. Ruijl, T. Ueda, J. A. M. Vermaseren, and A. Vogt, The five-loop beta function of Yang-Mills theory with fermions, J. High Energy Phys. 02 (2017) 090.

[30] F. Herzog, B. Ruijl, T. Ueda, J. A. M. Vermaseren, and A. Vogt, On Higgs decays to hadrons and the R-ratio at N^4LO, J. High Energy Phys. 08 (2017) 113.

[31] K. G. Chetyrkin, G. Falcioni, F. Herzog, and J. A. M. Vermaseren, Five-loop renormalisation of QCD in covariant gauges, J. High Energy Phys. 10 (2017) 179; 12 (2017) 006(A).

[32] S. Weinberg, Larger Higgs Exchange Terms in the Neutron Electric Dipole Moment, Phys. Rev. Lett. **63**, 2333 (1989).

[33] D. A. Demir, M. Pospelov, and A. Ritz, Hadronic EDMs, the Weinberg operator, and light gluinos, Phys. Rev. D **67**, 015007 (2003).

[34] W. Dekens, J. de Vries, J. Bsaisou, W. Bernreuther, C. Hanhart, U.-G. Meißner, A. Nogga, and A. Wirzba, Unraveling models of *CP* violation through electric dipole moments of light nuclei, J. High Energy Phys. 07 (2014) 069.

[35] T. Abe, J. Hisano, and R. Nagai, Model independent evaluation of the Wilson coefficient of the Weinberg operator in QCD, J. High Energy Phys. 03 (2018) 175; Erratum, J. High Energy Phys. 09 (2018) 20.

[36] Y. Chien, V. Cirigliano, W. Dekens, J. de Vries, and E. Mereghetti, Direct and indirect constraints on *CP*-violating Higgs-quark and Higgs-gluon interactions, J. High Energy Phys. 02 (2016) 011.

[37] V. Cirigliano, W. Dekens, J. de Vries, and E. Mereghetti, Constraining the top-Higgs sector of the standard model effective field theory, Phys. Rev. D **94**, 034031 (2016).

[38] J. Brod, U. Haisch, and J. Zupan, Constraints on *CP*-violating Higgs couplings to the third generation, J. High Energy Phys. 11 (2013) 180.

[39] J. Brod and E. Stamou, Electric dipole moment constraints on *CP*-violating heavy-quark Yukawas at next-to-leading order, arXiv:1810.12303.

[40] B. Graner, Y. Chen, E. G. Lindahl, and B. R. Heckel, Reduced limit on the permanent electric dipole moment of ^{199}Hg, Phys. Rev. Lett. **116**, 161601 (2016); Erratum, Phys. Rev. Lett. **119**, 119901(E) (2017).

[41] T. Chupp, P. Fierlinger, M. Ramsey-Musolf, and J. Singh, Electric dipole moments of the atoms, molecules, nuclei and particles, Rev. Mod. Phys. **91**, 015001 (2019).

[42] E. Braaten, C.-S. Li, and T.-C. Yuan, The Evolution of Weinberg's Gluonic *CP* Violation Operator, Phys. Rev. Lett. **64**, 1709 (1990).

[43] E. Braaten, C. S. Li, and T. C. Yuan, The gluon color—electric dipole moment and its anomalous dimension, Phys. Rev. D **42**, 276 (1990).

[44] N.-P. Chang and D.-X. Li, The evolution of Weinberg's gluonic *CP* operator and gauge dependence, Phys. Rev. D **42**, 871 (1990).

[45] R. D. Peccei and H. R. Quinn, *CP* Conservation in the Presence of Instantons, Phys. Rev. Lett. **38**, 1440 (1977).

[46] C. Itzykson and J. B. Zuber, *Quantum Field Theory*, International Series in Pure and Applied Physics (McGraw-Hill, New York, 1980).

[47] P. Pascual and R. Tarrach, QCD: Renormalization for the practitioner, Lect. Notes Phys. **194**, 1 (1984).

[48] J. A. Dixon and J. C. Taylor, Renormalization of Wilson operators in gauge theories, Nucl. Phys. **B78**, 552 (1974).

[49] S. D. Joglekar and B. W. Lee, General theory of renormalization of gauge invariant operators, Ann. Phys. (N.Y.) **97**, 160 (1976).

[50] G. 't Hooft, The background field method in gauge field theories, in *Functional and Probabilistic Methods in Quantum Field Theory. 1. Proceedings of the 12th Winter School of Theoretical Physics, Karpacz, 1975* (1975), pp. 345–369.

[51] B. S. DeWitt, A gauge invariant effective action, in *Proceedings of the Oxford Conference on Quantum Gravity Oxford, England, 1980* (1980), pp. 449–487.

[52] L. F. Abbott, The background field method beyond one loop, Nucl. Phys. **B185**, 189 (1981).
[53] L. F. Abbott, Introduction to the background field method, Acta Phys. Pol. B **13**, 33 (1982).
[54] W. Dekens and J. de Vries, Renormalization group running of dimension-six sources of parity and time-reversal violation, J. High Energy Phys. 05 (2013) 149.
[55] V. Cirigliano, E. Mereghetti, and P. Stoffer, Non-perturbative renormalization scheme for the *CP*-odd three-gluon operator, arXiv:2004.03576.
[56] A. A. Vladimirov, Method for computing renormalization group functions in dimensional renormalization scheme, Teor. Mat. Fiz. **43**, 210 (1980) [Theor. Math. Phys. **43**, 417] (1980).
[57] F. Herzog and B. Ruijl, Extension of the R*-method to arbitrary local QFTs (to be published).
[58] R. Beekveldt, M. Borinsky, and F. Herzog, The Hopf algebra structure of the R^*-operation, arXiv:2003.04301.
[59] P. Nogueira, Automatic Feynman graph generation, J. Comput. Phys. **105**, 279 (1993).
[60] S. A. Larin, The Renormalization of the axial anomaly in dimensional regularization, Phys. Lett. B **303**, 113 (1993).
[61] B. Ruijl, T. Ueda, and J. Vermaseren, FORM version 4.2, arXiv:1707.06453.
[62] G. 't Hooft and M. J. G. Veltman, Regularization and renormalization of gauge fields, Nucl. Phys. **B44**, 189 (1972).
[63] B. Ruijl, T. Ueda, and J. A. M. Vermaseren, Forcer, a FORM program for the parametric reduction of four-loop massless propagator diagrams, Comput. Phys. Commun. **253**, 107198 (2020).
[64] T. van Ritbergen, A. N. Schellekens, and J. A. M. Vermaseren, Group theory factors for Feynman diagrams, Int. J. Mod. Phys. A **14**, 41 (1999).
[65] M. Tanabashi *et al.* (Particle Data Group Collaboration), Review of particle physics, Phys. Rev. D **98**, 030001 (2018).
[66] W. E. Caswell, Asymptotic Behavior of Nonabelian Gauge Theories to Two Loop Order, Phys. Rev. Lett. **33**, 244 (1974).
[67] D. R. T. Jones, Two loop diagrams in Yang-Mills theory, Nucl. Phys. **B75**, 531 (1974).
[68] E. Egorian and O. V. Tarasov, Two loop renormalization of the QCD in an arbitrary gauge, Teor. Mat. Fiz. **41**, 26 (1979) [Theor. Math. Phys. **41**, 863 (1979)].
[69] O. V. Tarasov, A. A. Vladimirov, and A. Yu. Zharkov, The Gell-Mann-Low function of QCD in the three loop approximation, Phys. Lett. **93B**, 429 (1980).
[70] S. A. Larin and J. A. M. Vermaseren, The three loop QCD Beta function and anomalous dimensions, Phys. Lett. B **303**, 334 (1993).
[71] M. Rizik, C. Monahan, and A. Shindler, Renormalization of *CP*-violating pure gauge operators in perturbative QCD using the gradient flow, Proc. Sci., LATTICE2018 (**2018**) 215 [arXiv:1810.05637].
[72] R. Gupta, Present and future prospects for lattice QCD calculations of matrix elements for nEDM, Proc. Sci., SPIN2018 (**2019**) 095 [arXiv:1904.00323].
[73] V. Cirigliano, Z. Davoudi, T. Bhattacharya, T. Izubuchi, P. E. Shanahan, S. Syritsyn, and M. L. Wagman (USQCD Collaboration), The role of lattice QCD in searches for violations of fundamental symmetries and signals for new physics, Eur. Phys. J. A **55**, 197 (2019).
[74] U. Haisch and A. Hala, Sum rules for *CP*-violating operators of Weinberg type, J. High Energy Phys. 11 (2019) 154.
[75] A. Manohar and H. Georgi, Chiral quarks and the non-relativistic quark model, Nucl. Phys. **B234**, 189 (1984).
[76] J. de Vries, R. G. E. Timmermans, E. Mereghetti, and U. van Kolck, The nucleon electric dipole form factor from dimension-six time-reversal violation, Phys. Lett. B **695**, 268 (2011).
[77] M. D. Rizik, C. J. Monahan, and A. Shindler, Short flow-time coefficients of *CP*-violating operators, arXiv:2005.04199.
[78] C. Abel *et al.* (nEDM Collaboration), Measurement of the permanent electric dipole moment of the neutron, Phys. Rev. Lett. **124**, 081803 (2020).
[79] F. Krauss, S. Kuttimalai, and T. Plehn, LHC multijet events as a probe for anomalous dimension-six gluon interactions, Phys. Rev. D **95**, 035024 (2017).
[80] F. Maltoni, E. Vryonidou, and C. Zhang, Higgs production in association with a top-antitop pair in the standard model effective field theory at NLO in QCD, J. High Energy Phys. 10 (2016) 123.
[81] N. P. Hartland, F. Maltoni, E. R. Nocera, J. Rojo, E. Slade, E. Vryonidou, and C. Zhang, A Monte Carlo global analysis of the standard model effective field theory: The top quark sector, J. High Energy Phys. 04 (2019) 100.
[82] S. Alioli, W. Dekens, M. Girard, and E. Mereghetti, NLO QCD corrections to SM-EFT dilepton and electroweak Higgs boson production, matched to parton shower in POWHEG, J. High Energy Phys. 08 (2018) 205.
[83] B. Ruijl, F. Herzog, T. Ueda, J. A. M. Vermaseren, and A. Vogt, The R^*-operation and five-loop calculations, Proc. Sci., RADCOR2017 (**2018**) 011 [arXiv:1801.06084]; J. Phys. Conf. Ser. **1085**, 052006 (2018).